Artificial Thickening of High Subsonic Mach Number Boundary Layers

L. J. Otten III*
NASA Ames Research Center, Moffett Field, Calif.

and

J. T. Van Kuren†
Air Force Flight Dynamics Lab., Wright Patterson Air Force Base, Ohio

A wind-tunnel experiment was performed to examine the effect of turbulence enhancers on the growth of a flat-plate turbulent boundary layer. The freestream Mach number was varied from 0.6 to 0.9 with unit Reynolds numbers of 6.56×10^6/m and 13.12×10^6/m. Several configurations of high drag objects were mounted near the leading edge of a long flat plate to introduce momentum losses. Measurements of both mean and time variable flow parameters were made at downstream locations to quantify the influence of the turbulence enhancers. A configuration consisting of two parallel rows of alternately spaced, 0.317-cm diam cylinders that were 16 and 12 diam in length produced 1/9 to 1/7 power velocity profiles. Fluctuating total temperature, velocity, and static pressure profiles were found to be similar to natural turbulent boundary-layer profiles. The techniques presented here can be useful whenever thick turbulent boundary layers are required but where the natural growth of the layer is limited by the test facility.

Introduction

Background

FOR a number of ground-based aerodynamic investigations, it is desirable to conduct tests with boundary layers that are full scale. For example, large-scale diffuser or inlet studies[1] and, more recently, laser light transmission investigations, inherently require boundary layers that are relatively large. In evaluating the sources of a thick boundary layer, a wind tunnel wall boundary layer was rejected because of the difficulty in characterization and control associated with an upstream history of pressure gradients, wall curvatures, heat transfer, and, for most transonic flow facilities, mass transfer through a slotted test section. A natural flat-plate boundary layer was also rejected since, for any flat plate of reasonable length suspended in a wind tunnel, the boundary layer is relatively thin and the associated turbulence eddies are small compared to those existing in a full-scale aircraft boundary layer. The only practical alternative approach is to enhance the growth of the flat-plate boundary layer with artificial thickeners.

Artificial thickening of boundary layers has been the subject of sporadic investigation since the early 1950's. Klebanoff and Diehl[2] reported some early low speed ($u_\infty < 33$ m/sec where u_∞ = freestream velocity) artificial thickening effects. More recently, investigations have also been conducted at low speeds[3] or at supersonic speeds.[4,5] The objective of this investigation was to extend the artificial thickening effort to high subsonic speeds and to quantify the variations in both the mean and unsteady flow parameters for comparison to similar natural boundary-layer parameters.

Received Jan. 20, 1976: presented as Paper 76-51 at the AIAA 14th Aerospace Sciences Meeting, Washington, D. C., Jan. 26-28, 1976; revision received Aug. 10, 1976. The authors wish to thank K. R. Raman, D. Johnson, W. Rose, and D. Buell for their assistance in collecting the data reported in this paper.

Index categories: Boundary Layers and Convective Heat Transfer-Turbulent; Subsonic and Transonic Flow; Nonsteady Aerodynamics.

*Captain, AFSC Research Associate. Member AIAA.

†Aerospace Engineer. Associate Fellow AIAA.

To evaluate the effectiveness of the thickeners, certain criteria are required. For this investigation, the following criteria were applied: 1) there shall be no variations in mean flow parameters nor a velocity component in the crossflow direction parallel to the plate surface; 2) the mean velocity profile shall be approximately a power low profile with exponent between 1/4 and 1/9, depending on the Mach number and Reynolds number; 3) the frequency spectrum of fluctuating static pressure shall have a random distribution without discrete energy spikes; and 4) the measured fluctuating variables associated with a thickened layer shall agree with those measured in natural boundary layers.

Facility and Model

The tests reported here were performed in the NASA-Ames Research Center 1.83- by 1.83-m (6×6 ft) pressure tunnel. Tunnel Mach number was varied from 0.6 to 0.9 and the Reynolds number was maintained at either 6.57×10^6/m or 13.14×10^6/m. The test model was a flat plate 2.08 m long and 0.76 m wide (Fig. 1). The plate was mounted on the side of the tunnel on a center pylon far enough from the wall to insure that the plate was not immersed in the tunnel boundary layer. An elliptic leading edge, with the major axis four times the minor axis, was used to preclude separation and to reduce the mass flow and blockage beneath the plate. Pressure orifices on the lower surface of the plate always showed the flow between the plate lower surface and the tunnel wall to be subsonic. A 0.6 cm wide strip of No. 80 grit was placed 1 cm aft of the leading edge to ensure early and uniform transition to turbulent flow. Boundary-layer measurements were normally made over a 0.50- by 0.12-m surface, located on the centerline of the plate, 1.22 m aft of the leading edge. Surface instrumentation consisted of mean and unsteady static pressure transducers located both along and off the centerline.

The mean static pressure ports were connected to a Scanivale while the unsteady pressures were measured with 0.24-cm diameter solid-state, diaphragm-type transducers having a frequency response of 0 to 40 kHz. Measurement above the surface of the plate were made using a remotely controlled probe with a variety of instrumented tips. This probe was

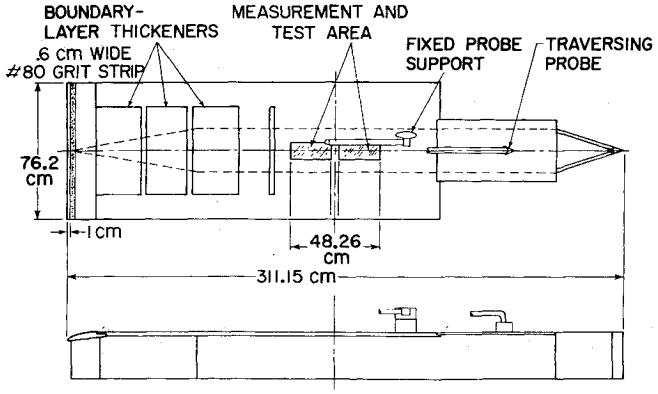

Fig. 1 General model layout, top and side view.

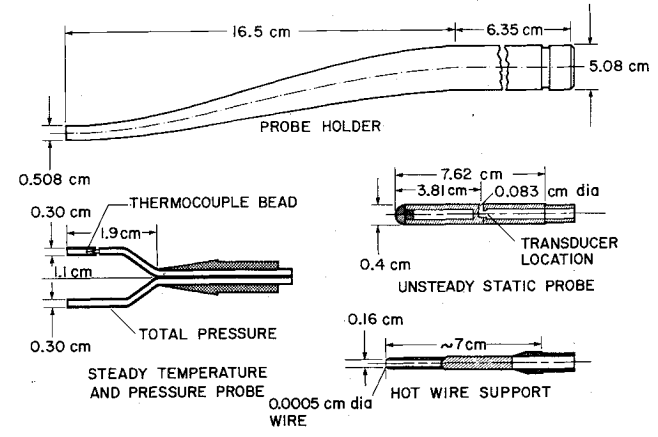

Fig. 2 Instrumentation holder and instrumented tips.

movable over a distance of 25 cm in the flow direction (x axis) and of 15 cm normal to the plate (z direction) with a resolution of better than 0.25 cm. Long, thin, tapered tip holders were used to reduce probe interference in the local area of the measurements. Figure 2 is a sketch of the holder and the instrumented tips. (The holder and the tips were designed by K. R. Raman of Raman Aeronautics, Research and Engineering.) As seen in Fig. 2, tips were made to hold a steady-state static orifice, an unsteady static pressure transducer, and a hot wire that functioned as a fluctuating total temperature transducer. Testing of the unsteady static probe showed that the fundamental Helmholtz resonance of the cavity was in excess of 25 kHz when the diaphragm of the pressure transducer was moved to a position 0.02 cm aft of the port. The hot wire used for the total temperature measurements was 0.0005 cm in diameter and 0.16 cm long. The Wollaston wire had a resistance of 5 to 7 Ω and a frequency response in excess of 50 kHz. Thermocouple data recorded during the test showed that the plate temperature followed the tunnel temperature to within a few degrees; a near adiabatic plate is therefore assumed.

The technique used to thicken the boundary layer was to introduce an added momentum deficit through the placement of cylindrical pins normal to the surface of the plate. The details of how the pins were designed are discussed later. Four variations of pin size and placement were tried (Fig. 3). The first configuration tested (configuration 2, with configuration 1 being the clean flat plate) was a series of three sets of upright pins, 1.27, 1.905, and 2.54 cm long and 0.32, 0.47, and 0.635 cm in diameter, respectively.[6] Each set consisted of between 8 and 13 rows of about 10 cylinders with the upstream row of each set being located at 17.3, 45.2, and 70.6 cm aft of the leading edge. The large number of pins was used to ensure thorough mixing of the shed vortices while the increase in size for each set was designed to equal the approaching thickened

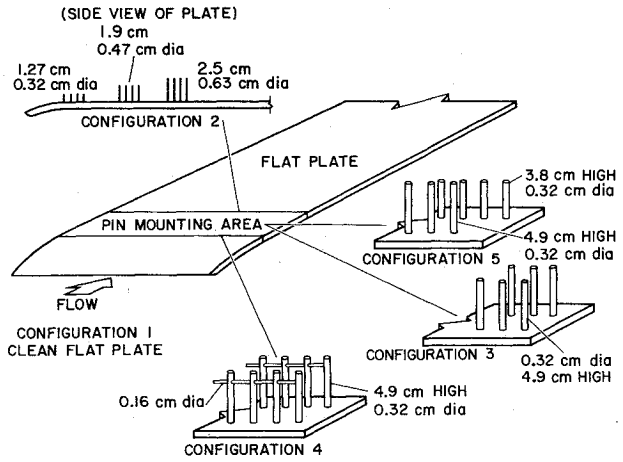

Fig. 3 Model configurations.

boundary-layer momentum thickness. Configuration 3 consisted of two rows of pins, nominally 0.317 cm in diameter and 4.9 cm long, mounted 17.3 and 19.2 cm aft of the leading edge. The remaining models were variations of configuration 3. In configuration 4, a horizontal row of 0.07-cm diam wire, tied between each of the pins in configuration 3, was used. This wire was 0.64 cm from the plate on the upstream row, and 1.27 cm from the plate on the downstream row; it was designed to add a momentum loss in the velocity profile observed in configuration 3. The last model consisted of two rows of nominal 0.317-cm diam pins, the first one being 4.9 cm long and the second one 3.8 cm long.

The coordinate system used is such that x is in the direction of the flow, y is parallel to the plate and normal to the flow direction, and the z axis is normal to the plate; z is measured positive toward the mainstream.

Pin Design

To create an artificially thickened boundary layer, it is necessary to reduce the momentum of the flow in a prescribed distribution above the surface. This can be done with a distribution of high drag objects sufficiently far upstream of the experimental region to allow for the momentum to equilibrate to a smooth distribution. One method for determining the size and placement of the high drag objects is to determine how much momentum must be removed from the flow to obtain the desired boundary-layer thickness and to then equate that to the drag of the blunt objects. Since the desired boundary layer was a turbulent boundary layer with a classical power-law profile, mean velocity profiles could be expressed by

$$u/u_\infty = (z/\delta)^{1/n} \tag{1}$$

where u is the local velocity in the stream wise direction, u_∞ is the freestream velocity, and δ is the z distance for $u = 0.98\,u_\infty$.[7] The drag per unit width of a boundary layer on a flat plate is

$$\text{Drag} = \rho_\infty u_\infty^2 \int_0^\delta \frac{\rho u}{\rho_\infty u_\infty}\left(1 - \frac{u}{u_\infty}\right) dz \tag{2}$$

where ρ and ρ_∞ are the local and freestream densities, respectively. By definition, the term under the integral is the momentum thickness, θ, so

$$\text{Drag} = \rho_\infty u_\infty^2\, \theta \tag{3}$$

Following the reasoning of Ref. 4, the thickness of the boundary layer can be increased by adding drag from objects in the flow. The added drag is

$$\text{Added drag} = \frac{\rho_\infty u_\infty^2}{2} C_D A \tag{4}$$

where C_D is the drag coefficient of the object, and A is the frontal area per unit width. If C_f is the skin friction coefficient, the momentum thickness can then be expressed as

$$\theta = \frac{1}{2}\left(C_D A + \int_o^x C_f \, dx\right) \tag{5}$$

Thus the momentum thickness becomes a linear function of the amount of drag added by an upstream disturbance if the integral in Eq. (5) is small.

Using Eq. (1), the drag per unit width for the boundary layer can be expressed as

$$\text{Drag} = \rho_\infty u_\infty^2 \left[\frac{n}{(n+1)(n+2)}\right]\delta \tag{6}$$

In an isentropic perfect gas, the compressible Bernoulli equation can be placed in the following form (as found in Ref. 8)

$$\frac{\rho}{\rho_\infty} = \left\{1 - \frac{\gamma-1}{2} M_\infty^2 \left[\left(\frac{u}{u_\infty}\right)^2 - 1\right]\right\}^{1/\gamma-1} \tag{7}$$

where γ is the specific heat ratio and M_∞ is the freestream Mach number. In terms of a power profile this becomes

$$\frac{\rho}{\rho_\infty} = \left\{1 - \frac{\gamma-1}{2} M_\infty^2 \left[\left(\frac{z}{\delta}\right)^{2/n} - 1\right]\right\}^{1/\gamma-1} \tag{8}$$

In the outer layer of a turbulent boundary layer, the transfer of mass, momentum, and energy across the layer is by the fluid mixing process and the thermodynamic process can be assumed locally isentropic. Under this condition, Eqs. (3) and (8) can be combined with Eq. (2) to obtain

$$\text{Drag} = \rho_\infty u_\infty^2 \int_o^\delta \left\{1 - \frac{\gamma-1}{2} M_\infty^2 \left[\left(\frac{z}{\delta}\right)^{2/n} - 1\right]\right\}^{1/\gamma-1} \times \left[\left(\frac{z}{\delta}\right)^{1/n} - \left(\frac{z}{\delta}\right)^{2/n}\right] dz \tag{9}$$

Let $z/\delta = m$, $\gamma = 1.4$, and $a = 1/n$, then Eq. (9) becomes

$$\text{Drag} = \rho_\infty u_\infty^2 \, \delta f_{a, M_\infty}(m) \tag{10}$$

where

$$f_{a, M_\infty}(m) = \int_o^1 [1 + 0.2M_\infty^2(1 - m^{2a})]^{2.5} (m^a - m^{2a}) \, dm \tag{11}$$

can be calculated numerically. This expression can now be equated to the momentum loss imposed by high drag objects, and a pin design parameter σ can be calculated. For circular cylinders this becomes

$$\sigma = NRh = \frac{\delta f_{a, M_\infty}(m)}{C_{D_{\text{cyl}}}} \tag{12}$$

where N = number of pins per unit width, R = pin radius, and h = pin height.

Using this pin design, a plot of predicted boundary layer thickness for a 1/7 and 1/9 power profile was calculated as a function of freestream Mach number using the pins of configuration 3; these data are shown in Fig. 4 as solid lines. The circled data points are the measured boundary-layer thickness. The agreement between predicted and measured heights indicates that the momentum loss technique just described is applicable to high subsonic flow if compressibility is accounted for.

Decay Of Wakes

Discrete disturbances from the pins must be damped out by the time the flow reaches the measuring station if the artifically thickened layer is to be similar to a natural boundary layer. Reference 7 (p. 494) gives the following expression for the decay wakes behind two-dimensional bodies:

$$\frac{u'}{u_\infty} = \frac{(10)^{1/2}}{18\beta}\left(\frac{x}{C_D d}\right)^{-1/2} \tag{13}$$

where u' is the unsteady velocity, d is the body diameter, and $\beta = 0.18$. For an $x/d = 416$ and $C_D = 1.29$ (Ref. 9), such as was the case in this model, u'/u should be less than 5%. The conclusion is that either very long distances are required or very small diameters must be used to completely mix the wakes.

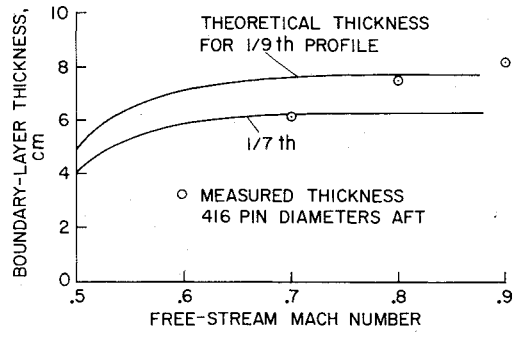

Fig. 4 Boundary-layer thickness as function of freestream Mach number.

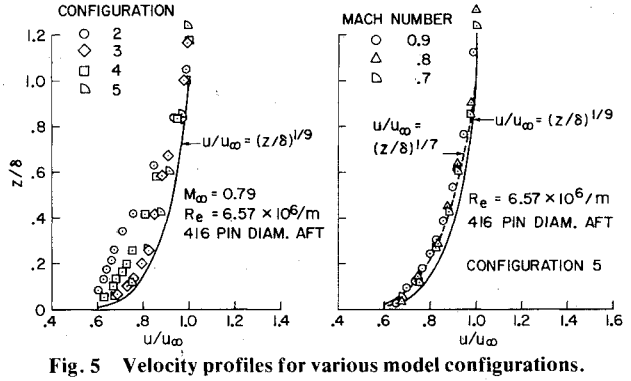

Fig. 5 Velocity profiles for various model configurations.

Results

In comparing the artifically thicknened layer to a natural boundary layer, velocity profiles and surface static pressure data were used to evaluate momentum addition and two-dimensionality. Fluctuating static pressure, total temperature, and streamwise velocity are used to quantify perturbation decay. All boundary-layer thicknesses are made nondimensional by δ. Values for δ were obtained by fitting a polynomial to the data by means of least squares. The order of the polynomial was chosen to minimize the mean deviation of the data. Spatial presentation of surface pressure data has been normalized by a pin diameter of 0.317 cm.

Using the approach suggested by Klebanoff and Diehl,[2] mean velocity profiles were used as a basis for initial comparison of various thicknesses. Figure 5 shows the variation in mean velocity profiles for each configuration tested. The freestream Mach number is 0.79 and the profiles are shown for a station located 470 pin diameters from the leading edge.

The dependence of the mean velocity profile on Mach number is also shown in Fig. 5, where data for a Mach number range of 0.7 to 0.9 are presented. The velocity profiles maintain their power profile characteristics over the investigated Mach number region. Using these data, it is concluded that a momentum loss mechanism such as configuration 5 will generate thickened turbulent boundary layers that have power-law, mean velocity profiles approximately 400 pin diameters downstream at high subsonic freestream velocities. A factor of 4.7 enhancement in the thickness of the boundary layer was realized with this configuration.

Table 1 Boundary-layer parameters (490 pin diameters downstream)

Configuration	Mach number	R_N/m	δ^*(cm)	θ (cm)	H
1	0.78	6.57×10^6	0.43	0.32	1.34
1	0.70	6.57×10^6	0.43	0.32	1.34
2	0.78	6.57×10^6	1.69	0.86	1.98
3	0.90	6.57×10^6	1.62	1.00	1.61
3	0.80	6.57×10^6	1.40	0.93	1.51
3	0.70	6.57×10^6	1.31	0.88	1.49
4	0.79	6.57×10^6	1.67	1.04	1.61
5	0.79	6.57×10^6	1.51	0.90	1.67
5	0.79	6.57×10^6	1.32	0.86	1.53
5	0.70	6.57×10^6	1.18	0.80	1.47
5	0.90	13.14×10^6	1.48	0.93	1.59
5	0.69	13.14×10^6	1.16	0.79	1.46

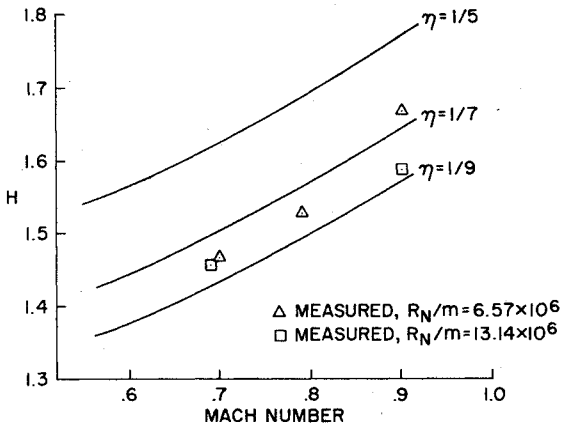

Fig. 6 Velocity profiles for configuration 5 and $0.7 \le M_\infty \le 0.9$.

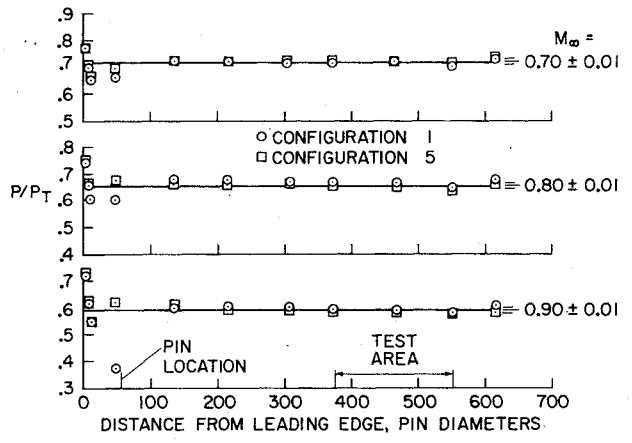

Fig. 7 Steady-state surface static pressures along centerline for $0.7 \le M_\infty \le 0.9$.

An additional indicator of a properly established turbulent boundary layer is the ratio of mass displacement thickness to momentum thickness, $H=\delta^*/\theta$, which is called the shape factor. For incompressible turbulent boundary layers on adiabatic flat plates, the experimentally measured shape factors[7] are approximately 1.34 ± 0.05. For higher freestream Mach numbers and nonadiabatic walls, the shape factor is a nonanalytical function of Mach number, wall-to-freestream temperature ratio, and the exponent of the velocity profile. Hunt and Sibulkin[10] have shown that a good approximation to H for the general case can be obtained from an analytical expression which is linear in the parameter $m=[(\gamma-1)/2]M_e^2$ where γ is the ratio of specific heats and M_e is the boundary layer outer edge Mach number. The case at hand can be approximated by a thermally insulated surface, such as the one treated theoretically by Tucker,[11] which shows a variation in reciprocal velocity exponent from 5 to 11 for Reynolds numbers from 10^4 to 10^9. In the range of Mach and Reynolds numbers covered in these tests, the experimental data for configuration 5 (Table 1) agree with the theoretical results of Tucker for a velocity exponent that is approximately between 1/7 and 1/9 (Fig. 6). These exponents also agree with those measured for the thickened layer. It can be concluded that the integral parameters of the thickened boundary layer agree with theoretical and experimental results of natural turbulent boundary layers.

Agreement between surface mean static pressures with and without the artificial turbulence generators was used to measure two-dimensionality of the flow. Freestream total pressure P_T has been used to make these data dimensionless. Figure 7 shows that, except for an area near the pins, the thickened flow has the same variation in surface static pressure as the clean flat plate. Variations in pressure in the aft region of the test area are associated with the probe holders and were not present when the holders were removed. The local Mach number generally varied $\pm2\%$ over the test area.

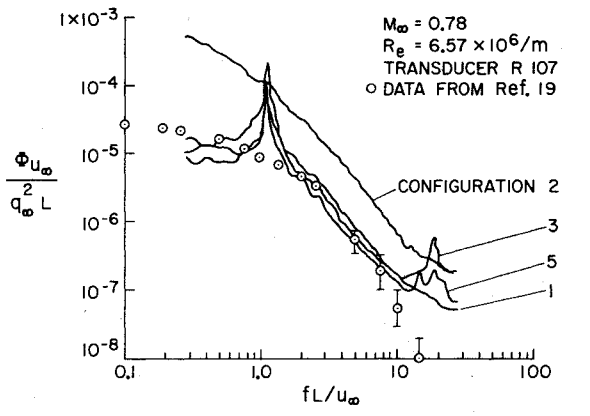

Fig. 8 Power spectra density for transducer located at 372.8 diameters downstream.

An evaluation of the effect that the thickeners had on the fluctuating surface static pressure required the use of a power spectra analysis because of a high tunnel noise level.[12] Figure 8 compares the static pressure power density spectra of most configurations for $M_\infty=0.78$ and $Rn=6.65\times10^6$/m. Because the spectra were virtually unchanged for each surface unsteady static transducer, only data from a transducer locate 373 pin diameters aft of the leading edge are shown. The spectra have been made dimensionless by using a reduced frequency based on unit length L for the frequency, and by multiplying the power squared per Hertz by $u_\infty/q_\infty L$, where q_∞ is the freestream dynamic pressure.

The large spike at a $fL/u=1.2$ represents the tunnel noise and agrees very well with the discrete frequency seen in Buell's data in the clean tunnel.[12] Since the rms static pressure is sim-

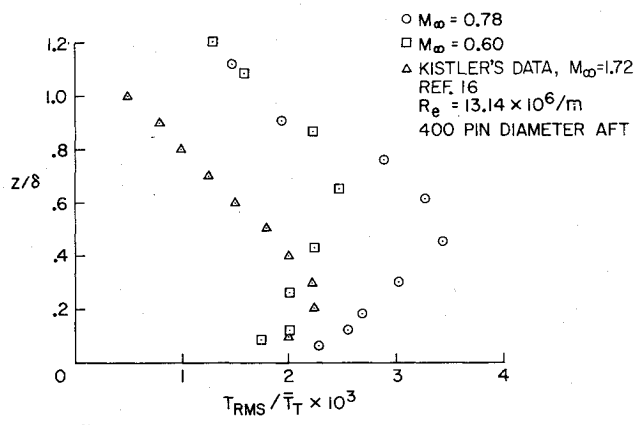

Fig. 9 Unsteady total temperature, configuration 5.

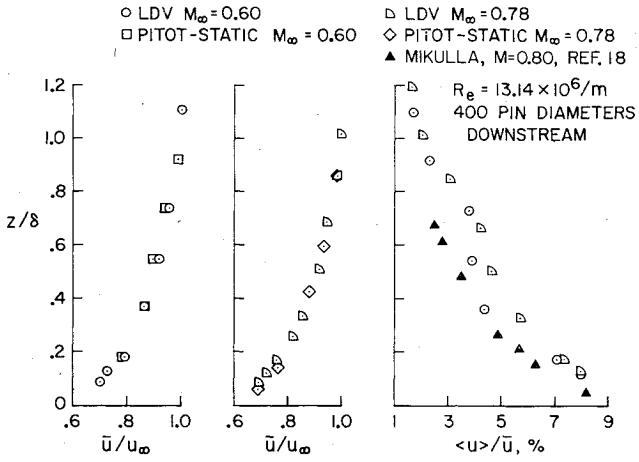

Fig. 10 Artifical thickened boundary-layer velocities, configuration 5.

ply the integral of the spectra, it is obvious that the energy in the spikes will dominate the integral. This, in turn, accounts for the small differences observed in the rms static pressures for the various configurations. The other set of spikes at the higher frequencies is associated with the artificial thickeners. The energy at these frequencies is low compared to the lower frequency energy, indicating that the pressures are well damped after traveling 400 pin diameters downstream.

Power spectra taken for configuration 2 reflect the very large number and varied length of the pins. The large number of pins increases the disturbance and causes the spectra to be generally higher, while the many pin lengths and close spacing cause these disturbances to be well mixed. With the exception of this multipin configuration, the static pressure spectra for the artifically thickened layers agree with the flat plate spectra, configuration 1. A second comparison to a natural boundary layer can be made by using the data from Ref. 13 (plotted as the circled points in Fig. 8). In reducing these data, the convective velocity was assumed to be 0.8 u_∞ and a rms static pressure coefficient of 0.006 was used. The agreement between this natural boundary layer and boundary layers thickened in the manner discussed here is quite good up to about 17,000 Hz, if the tunnel noise is ignored.

Hot wire measurements of the total temperature fluctuations through the pin-induced bounary layer are shown in Fig. 9. For both the $M_\infty = 0.78$ and $M_\infty = 0.60$ flows, the unsteady temperatures increase from a low level near the wall to a maximum at $z/\delta = 0.6$ and then return to a low level ($T_{rms}/\bar{T} = 0.012$) outside the layer. Sandborn[14] points out that considerable variation is observed for temperature fluctuation measurements in compressible flows. Recent results of Laderman and Demetriades[15] show that peak temperature

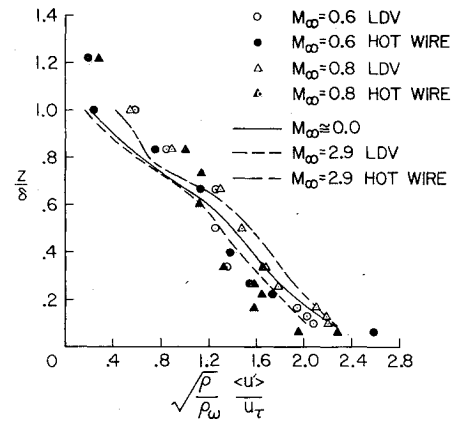

Fig. 11 Fluctuating velocity in boundary-layer expressed in similarity coordinates.

fluctuations are extremely sensitive to wall temperature. The peak fluctuations measured in these tests were within a factor of 2 of those reported by Kistler[16] and correspond to the cooled wall results interpolated from Laderman and Demetriades.[15] From the data of Fig. 9, it can be concluded that the pins do not seriously affect the fluctuating total temperature. In Fig. 9, T_{rms} is the root mean square of the fluctuating total temperaure and $\bar{T}$ is the mean local total temperature.

Velocity fluctuations through the thickened boundary layer were obtained using a laser doppler velocimeter described in Ref. 17. Figure 10 compares the mean velocity obtained from the velocimeter and the pitot probe and also shows the fluctuating freestream velocity as measured with the velocimeter. The fluctuating velocity in the artificial layer to the fluctuations found in a natural layer can be found in Fig. 7 of Ref. 17; that figure is included here as Fig. 11. Here, the unsteady velocity for the artificial boundary layer is presented in similarity coordinates and is seen to compare favorably with earlier data taken from $M_\infty = 0.0$ to 2.9.[17,18] In Fig. 11, σ_w is the wall density and u_τ is the friction velocity. These data (Figs. 10 and 11) indicate that the velocity disturbances introduced by the upstream pins have dissipated and that the thickened layer has flow characteristics similar to those of a natural flat plate boundary layer.

Conclusions

The thickening of turbulent boundary layers by means of thin upright cylinders can be accomplished at high subsonic Mach numbers using the techiques presented here. It is possible to reasonably predict the height of a thickened layer using a simple momentum loss technique which, in turn, allows one to choose a cylinder size and spacing for any desired thickness. By using small cylinders, the turbulence intensity of the disturbed flow can settle to normal boundary-layer levels within reasonable flow lengths with boundary layer thickness increased to desired values. Both mean and time variable flow quantities for an aritifically thickened boundary layer have been shown to resemble those of a natural turbulent boundary layer at approximately 400 pin diameters downstream; therefore, they satisfy the criteria chosen for turbulent boundary-layer characterization. The techniques presented here can be useful whenever thick turbulent boundary layers are required but where test facilities prevent the natural boundary layer from growing to the desired thickness.

References

[1] Samanick, N. E., Barnett, D. O., and Salmi, R. J., "Effect of External Boundary Layer on Performance of Axisymmetric Inlet at Mach Numbers of 3.0, and 2.5," NACA TM X-49, Sept. 1959, NACA.

[2]Klebanoff, P. S. and Diehl, Z. W., "Some Features of Artificially Thickened Fully Developed Turbulent Boundary Layers with Zero Pressure Gradient," NACA, Rept. 1110, 1954.

[3]Sajben, M., Kroutil, J. C., Hoffman, G. H., and Sedrick, A., "Generation of Velocity Profiles Using Sources of Nonuniform Solidity," *AIAA Journal*, Vol. 13, April 1975, pp. 417-418.

[4]Johnson, D. F. and Mitchell, G. A., "Experimental Investigation of Two Methods for Generating an Artifically Thickened Boundary Layer," NASA, TM X-2238, April 1971.

[5]Clever, W. W., "Results of an Experimental Turbulent Boundary Layer Control Investigation," NASA, TM X-53,899, Sept. 1969.

[6]Snyder, C. D., Private communications, McDonnell Douglas Aircraft Co., St. Louis, Mo. 1975.

[7]Schlitcting, H., *Boundary Layer Theory*. First English Ed., Pergamon Press, N. Y. 1955.

[8]Ames Research Staff, "Equations, Tables and Charts for Compressible Flow," NACA, Rept. 1135, 1953.

[9]Hoerner, S. F., *Fluid Dynamic Drag*, Published by the author, Midland Park, N. J.,1965.

[10]Hunt, B. L and Sibulkin, M., "Approximate Expression for the Boundary Layer Shape Factor," *AIAA Journal*, Vol. 3, Nov. 1965, pp. 2159-2160.

[11]Tucker, M., "Approximate Turbulent Boundary Layer Development in Plane Compressible Flow Along Thermally Insulated Surfaces with Application to Supersonic Tunnel Contour Corrections," NACA, TN 2045, March 1950.

[12]Buell, D. A., "An Experimental Investigation of the Air Flow Over a Cavity with Antiresonance Devices," NASA, TN D-6205, March 1971.

[13]Chaump, L. E., Martellucci, A., and Monfort, A., "Aeroacoustic Loads Assoicated with High Bet Reentry Vehicles," Air Force Flight Dynamics Lab., Wright-Patterson AFB, Ohio, AFF-DL-TR-72-138, Vol. I, AFFDL, May 1973.

[14]Sandborn, V. A., "A Review of Turbulence Measurements in Compressible Flow," NASA, TM X-62,337, March 1974.

[15]Laderman, A. J. and Demetriades, A., "Turbulent Fluctuations in the Hypersonic Boundary Layer Over an Adiabatic Slender Cone," *The Physics of Fluids*, Vol. 19, March 1976, pp. 121-144.

[16]Kistler, A. L., "Fluctuation Measurements in a Supersonic Turbulent Boundary Layer," *The Physics of Fluids*, Vol. 2, May-June 1959, pp. 290-296.

[17]Johnson, D. A. and Rose, W. C., "Turbulence Measurements in a Transonic Boundary Layer and Free Shear Flow Using Laser Velocimeter and Hot Wire Anemometer Techniques," AIAA Paper 76-399, 1976, 9th Fluid and Plasma Dynamics Conference, San Diego, Calif.

[18]Horstman, C. C. and Rose, W. C., "Hot Wire Anemometry in Transonic Flow," NASA, TM X-62,495, Dec. 1975.